Mapping Topsoil Organic Carbon Stocks in Grand-Duchy of Luxembourg

Antoine Stevens & Bas van Wesemael
Georges Lemaître Centre for Earth and Climate Research,
Earth and Life Institute,
3 Place Pasteur - 1348 Louvain-la-Neuve,
Belgium
email: antoine.stevens@uclouvain.be

Simone Marx & Lionel Leydet
Ministère de l'Agriculture, de la Viticulture et de la Protection des consommateurs,
Administration des services techniques de l'agriculture,
Service de Pédologie,
72, avenue L. Salentiny - 9080 Ettelbruck,
Grand Duchy of Luxembourg
email: simone.marx@asta.etat.lu

October 7, 2014

1 Introduction

We have previously estimated the Organic Carbon (OC) content (or concentration) of topsoils of the Grand-Duchy of Luxembourg (GDL) [1]. However, when assessing the amount of OC stored in soils of a given area, account has to be taken of the soil density, soil depth and proportion of fine earth to the total soil mass. Soil OC stocks can be computed according to Eq. 1 :

$$OC_s \left[t\, ha^{-1}\right] = \frac{d\,[cm] \times OC_c \left[g\, kg^{-1}\right] \times BD \left[g\, cm^{-3}\right] \times (1 - RM) \left[g\, g^{-1}\right]}{10} \quad (1)$$

where OC_s are the OC stocks, d is the depth over which stocks are computed, OC_c is the OC content in the fine earth fraction (< 2 mm) of the soil in the 0-d cm layer , BD is the bulk density or the dry weight of soil divided by its volume and RM is the mass proportion of rock fragment in the total mass of soil. The aim of this study is to map OC stocks of GDL in the 0-30 cm layer by combining continuous spatial layers representing OC content, BD and RM. In the next sections, we describe how these variables and associated errors are derived.

2 OC content in the 0-30 cm layer

Soil samples in each land cover were collected with different methodologies and over different sampling depth [1]: 0-25 cm in croplands, 0-10 cm in grasslands, 0-20 and 20-40 cm in forest and 0-30 cm in vineyards. The OC content of cropland, grassland and forest soils has therefore to be corrected to represent the mean OC content over a standard depth of 0-30 cm. To achieve this, the vertical distribution of OC in the soil profile should be known or modeled. Generally speaking, OC content decrease with depth and the shape of the relationship between OC and depth depends on several factors, the most important being land use, OC content in the top and bottom of the profile, and soil type (texture and drainage) [2, 3, 4]. Forest soils tends to have the highest rate of decline with depth compared to cropland and grassland soils due to the lower root to shoot ratio resulting in a high input of organic matter by plant litter [3]. OC content in croplands is more or less constant in the tillage layer and is distinctly lower than grasslands and croplands at the same depths. The vertical distribution of OC can be modeled by splines [5] or exponential decay functions [3] but other relations can be used, such as those based on a conceptual model of pedogenesis [4].

Cropland and grassland soils. To model the OC distribution with depth, we used data from BDSOL1964-1973 database (see [1] for details on this database) containing OC analyses of soil profiles collected in GDL (Figure 1). Since in BDSOL, data represent averages per horizon, we generated first a continuous OC distribution with depth using mass-preserving splines [6, 5] as implemented in the GSIF R package [7]. Mass-preserving splines allow fitting functions that preserve the mean value per horizon by ensuring that the area to the left of the fitted line above the horizon depth average is equal to the area to the right below the horizon depth average [6]. The λ parameter controlling the degree of smoothness of the splines was set to 0.1 and chosen as to obtain a low root mean square error of prediction while keeping the functions smooth enough (Figure 2). Based on the fitted splines, we computed the average OC content for the 0-30 cm layer(OC_{30}), for the 0-10 cm layer for grasslands (OC_{10}) and for the 0-25 cm layer for croplands (OC_{25}). Then, we simply modeled OC_{30} as a function of OC_{10} for grasslands and OC_{25} for croplands. In croplands, a linear relationship fits very well to the data ($r^2 = 0.99$) and shows that OC_{30} is about 94 % of OC_{25} (Figure 3). In grasslands, the relationship between OC_{30} and OC_{10} is non-linear and we found the best fit with a square root transformation of OC_{10} ($r^2 = 0.89$; Figure 4) . This relationship suggests that the rate of OC decline in grasslands is more pronounced for soils with high OC content in the top of the profiles. While the fit is less good as for croplands, we found no indications that the relationship is dependent of other factors such as texture. This can be expected since texture seems generally to play a role only at lower depths in the profiles [2].

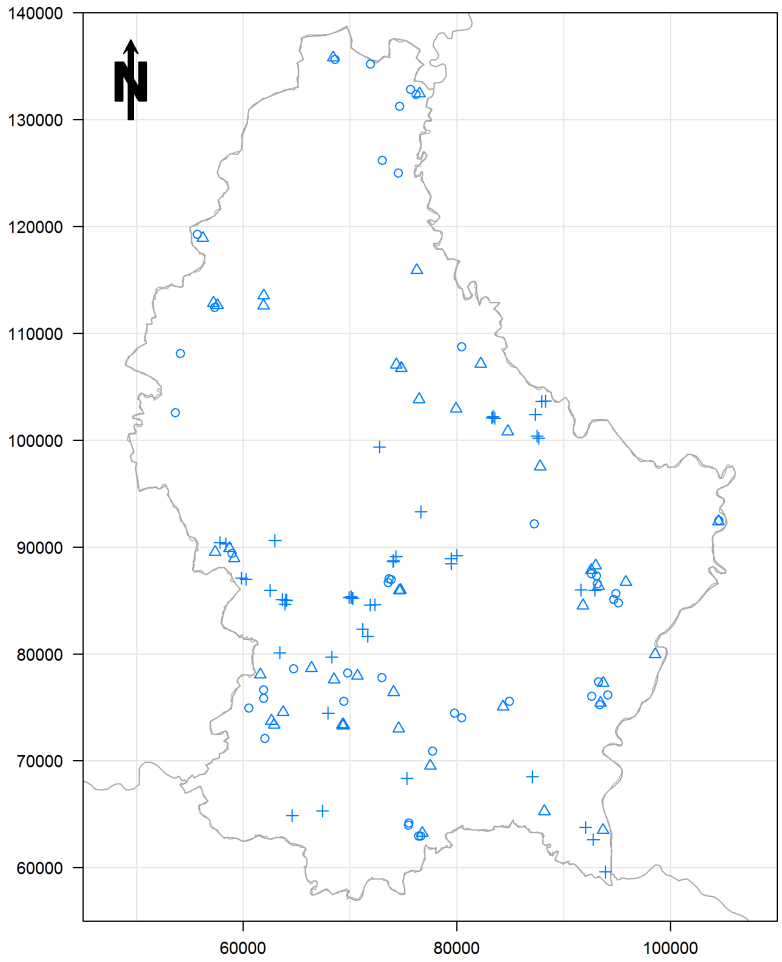

Figure 1: Location of soil profiles (i) under cropland (o) and grassland (△) land cover in BDSOL1964-1973 and (ii) in BDSOL2009-2013 (+).

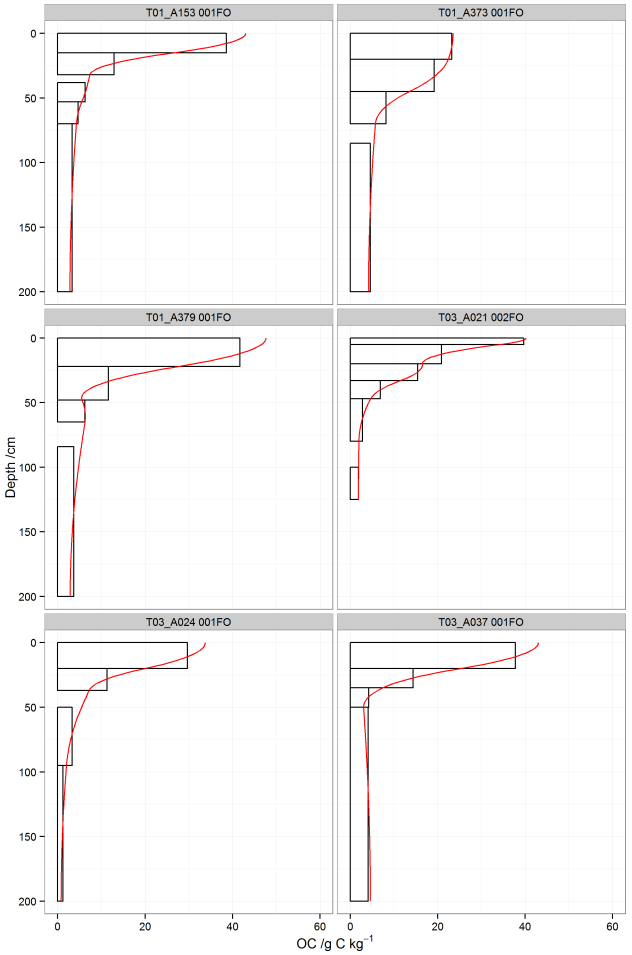

Figure 2: Examples of soil profiles showing horizon observed OC values (g C kg^{-1}; horizontal bars) and interpolated OC values using mass-preserving splines (red lines).

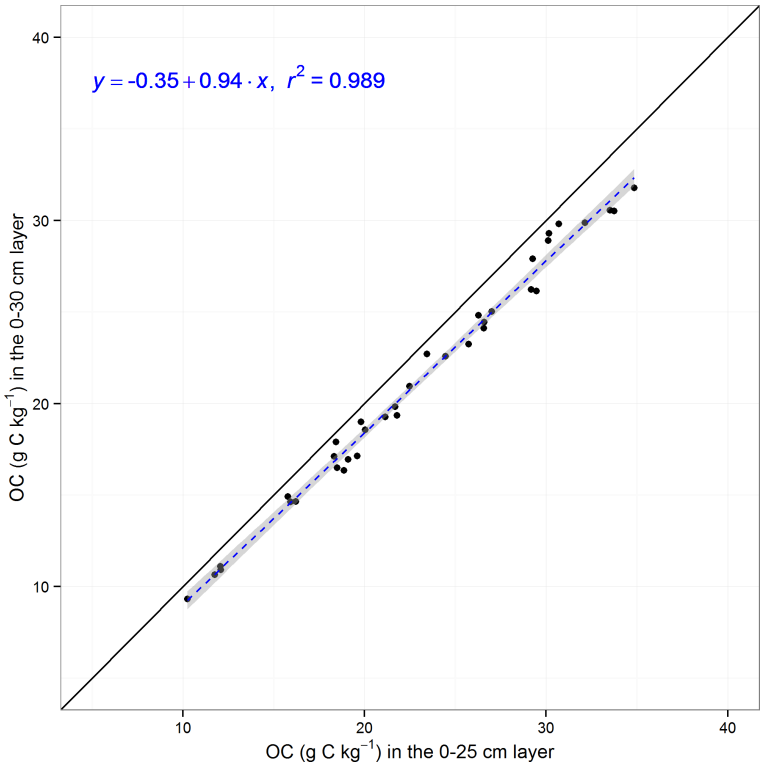

Figure 3: OC content (g C kg^{-1}) in the 0-30 cm layer as a function of OC content (g C kg^{-1}) in the 0-25 cm layer in cropland soil profiles with a linear trend line (blue dashed line). The black line indicate the 1:1 line.

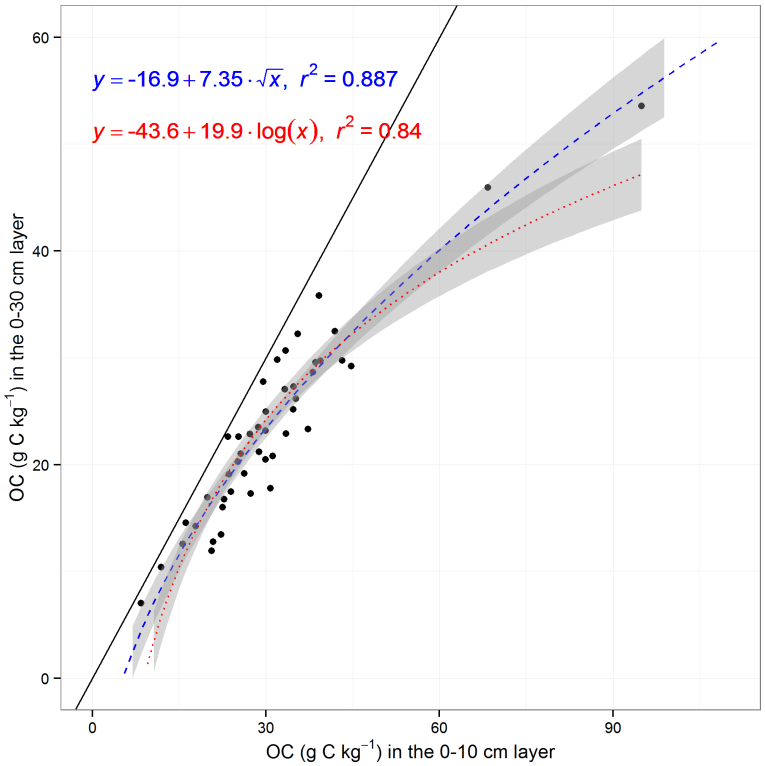

Figure 4: OC content (g C kg^{-1}) in the 0-30 cm layer as a function of OC content (g C kg^{-1}) in the 0-10 cm layer in grassland soil profiles with a log (red dotted line) and square root (blue dashed line) fit. The black line indicate the 1:1 line.

Forest soils. Since for forest soils, OC data for the 0-20 cm layer (OC_{20}) and the 20-40 cm layer (OC_{40}) were available, we followed a different approach than for the two other land covers. To estimate OC_{30}, we corrected OC values of the second horizon to represent OC in the 20-30 cm layer ($OC_{20\text{-}30}$) and computed the weighted mean of OC_{20} and $OC_{20\text{-}30}$. To computed $OC_{20\text{-}30}$, we fitted a linear regression through OC_{20} and OC_{40}as expressed in :

$$OC\left(z\right) = \beta_0 + \beta_1 \cdot z \tag{2}$$

and computed the mean OC content by integration of Eq. 2:

$$OC_{20-30} = \frac{\int_{20}^{30} OC\left(z\right) dz}{10} \tag{3}$$

OC map. After correction, the OC content was modeled separately for each land cover class using Generalized Additive Models (GAM) and soil covariates following the same methodology as described in [1]. The same covariates were selected by the stepwise backward procedure anad the models were very similar to the ones developed on non-corrected OC data (Appendix A). The GAM models were then used to create a map of OC content and standard errors of OC predictions.

3 Bulk density

When not measured, BD is generally modeled by a Pedo-Transfer Function (PTF) through its relation with Organic Matter (OM) and soil texture [8]. Several published PTFs predicting the bulk density of soils could be used, of which the PTF of Adams [9] (Eq. 4) Rawls [10] (Eq. 5), De Vos-Rawls [8] (Eq. 6) and De Vos [8] (Eq. 7).

$$BD_p = \frac{100}{\left(OM/0.311\right) + \left(100 - OM\right)/1.47} \tag{4}$$

$$BD_p = \frac{100}{\left(OM/0.224\right) + \left(100 - OM\right)/BD_m} \tag{5}$$

$$BD_p = \frac{100}{\left(OM/0.312\right) + \left(100 - OM\right)/1.661} \tag{6}$$

$$BD_p = 1.775 - 0.173\sqrt{OM} \tag{7}$$

BD_p is the predicted bulk density (g cm^{-3}), OM is the organic matter content (assuming a conversion factor of 1.724 with OC), and BD_m is the bulk density of the mineral fraction (see [11] for values of BD_m adapted for Belgian conditions). To evaluate the accuracy of published PTFs, we used a database of 51 soil profiles collected in 2009-2013 in Gutland (Figure 1). This database, hereafter called BDSOL2009-2013, contains notably OC, texture and BD measurements per soil horizons. We found the best fit with observed data with the PTF of De Vos (Eq. 7) showing an r^2 of 0.515 (Figure 5). The BD map was therefore produced by applying the PTF of De Vos to the predicted OC map (Figure 6). The prediction error of BD includes the prediction error of the PTF itself plus the error associated with the OC prediction as the independent variable in Eq. 7 [12]. The total error (expressed as Standard Errors - SE) associated with PTF-based estimates of BD_p was estimated by:

$$SE^2_{BDp}tot \quad = \quad SE^2_{BDp} + \left(\frac{\partial BD_p}{\partial OC_c}\right)^2 \cdot SE^2_{OCc} \tag{8}$$

and inserting Eq. 7 in Eq. 8 gives:

$$SE^2_{BDp}tot = SE^2_{BDp} + \frac{1}{4}\,0.173^2 OC_c^{-1} \cdot SE^2_{OCc} \tag{9}$$

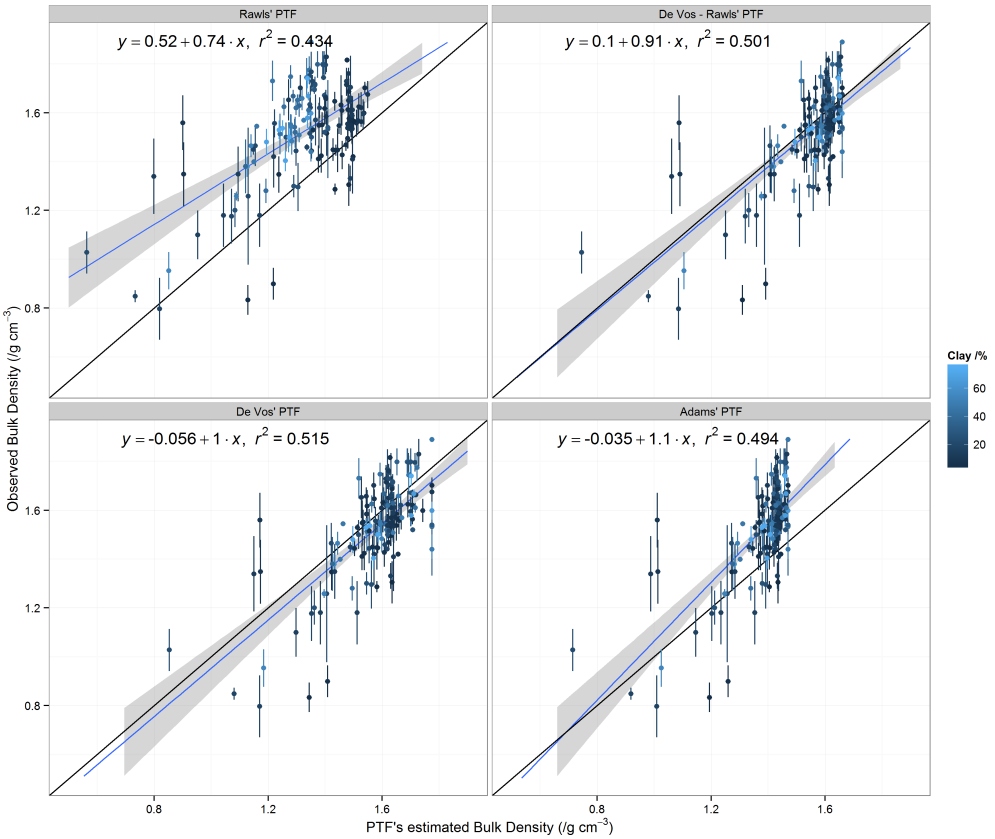

Figure 5: Observed bulk density (/ g cm^{-3}) *vs* bulk density estimated by PTFs. The error bars represent the standard deviation of the BD measurements.

4 Rock mass

The BDSOL2009-2013 database includes RM data. To produce the map of RM (g g^{-1}) and associated errors, we first extracted the top horizons of the soil profiles in the database. Then, we computed the mean RM content and standard error of the mean per soil association (Table 1; see [1] for details on the soil associations) and assigned the obtained values to the map of soil associations.The Oesling is covered by soils having a high RF content (21% composed of mainly shales; Table 1). RM content is also relatively high in the Bundsandstein and Dolomies du Muschelkalk compared to other soil associations of Gutland (Table 1).

Soil association	Mean	Standard Error	n
Oesling	21.59	1.19	111
Buntsandstein	9.44	2.92	19
Dolomies du Muschelkalk	6.35	0.89	32
Calcaires du Bajocien	0.73	0.53	6
Grès de Luxembourg	1.00	0.22	85
Dépôts limoneux sur Grès	2.85	0.38	92
Argiles du lias inf. et moyen	4.32	0.36	153
Argiles lourdes du Keuper	3.48	0.55	68
Argiles lourdes des schistes bitumineux	1.83	0.61	29
Autres	3.10	0.69	96
	3.98	0.78	23

Table 1: Rock fragment content (%) per soil association classes

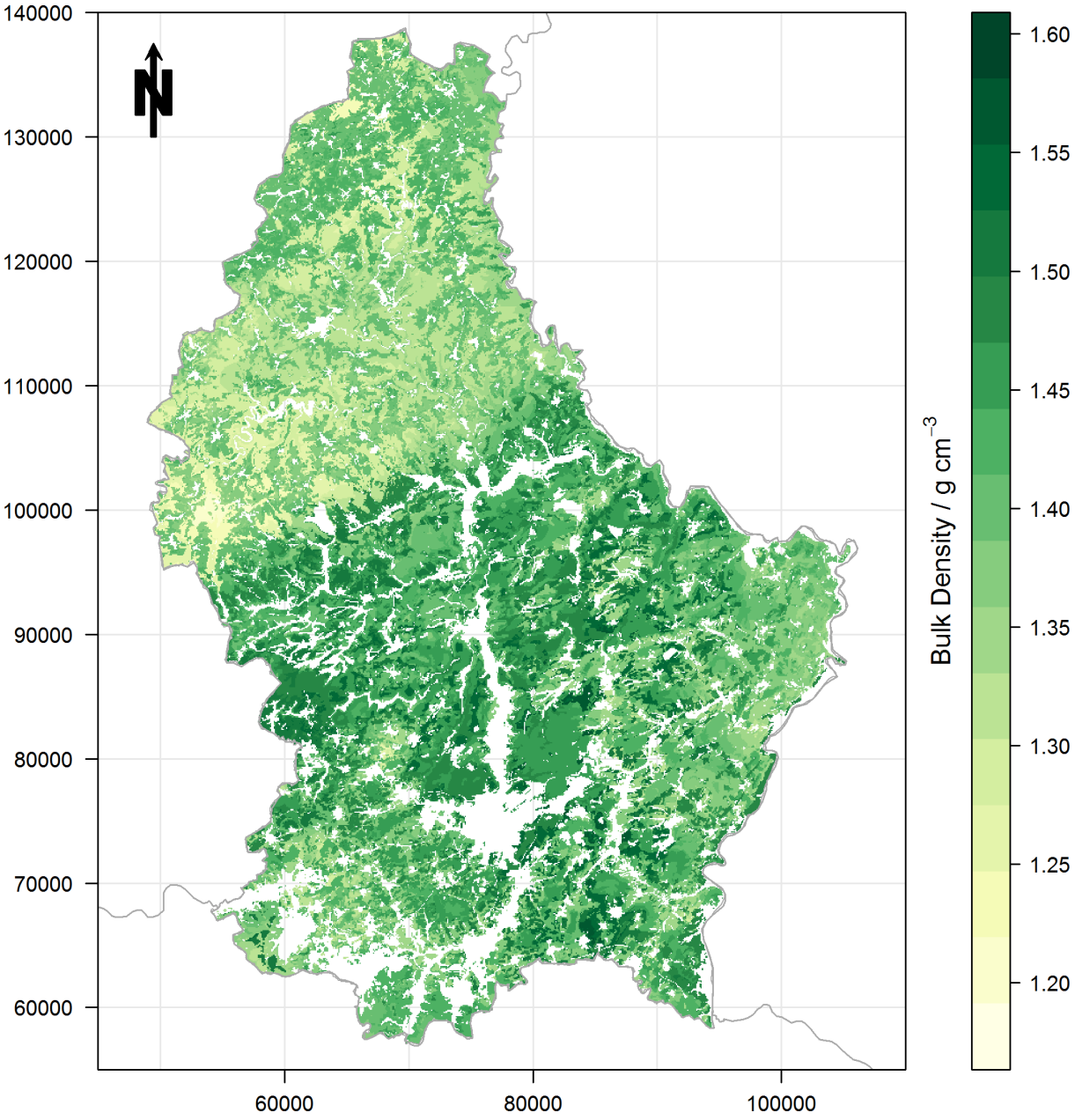

Figure 6: Bulk density (g cm^{-3}) as estimated by the calibrated PTF.

5 OC stocks

The map of OC_s was simply obtained by multiplying maps of OC_c, BD and RM according to Eq. 1. We derived the standard error of prediction of the stocks SE_{OCs} for each pixel using the error propagation formula based on a linear Taylor series expansion taking into account the covariance $s_{OCc,BD}$, $s_{OCc,1-RM}$ and $s_{BD,1-RM}$ of the variables in Eq. 1 [13]:

$$SE^2_{OCs} = OC^2_s \times \left[\frac{SE^2_{OCc}}{OC^2_c} + \frac{SE^2_{BDp}}{BDp^2} + \frac{SE^2_{RM}}{(1-RM^2)} + 2\,\frac{s_{OCc,BD}}{OC_c \times BD} - 2\,\frac{s_{OCc,1-RM}}{OC_c \times (1-RM)} - 2\,\frac{s_{BD,1-RM}}{BD \times (1-RM)} \right] \quad (10)$$

The obtained OC_s and SE_{OCs} map are shown in Figure 7 and 8. The map of OC_s strongly reflects the patterns already observed for OC_c [1]. High OC stocks in the 0-30 cm layer can be found in forest of Oesling (mean = 134 t C ha^{-1}) and grasslands of Gutland (mean = 113 t C ha^{-1}), while relatively low values are obtained for cropland (mean = 66 t C ha^{-1}) and vineyards (74 t C ha^{-1}) in the Gutland (Figure 9; Table 5-7). The mean OC_s over the entire GDL territory[1] is 101 ± 13 t C ha^{-1}, a relatively high value reflecting the high proportion of forest in GDL (ca. 37 %). The total OC stock is evaluated at 21.4 ± 7 Mt C. The validity of the OC_s map was checked with the samples of the BDSOL2009-2013 database. We should note that this exercise will not give a completely correct picture of the map accuracy because (i) the support of the validation data (i.e. soil profiles) may differ from the support of the calibration samples (e.g. fields for croplands) and (ii) the locations of the validation samples are not the result of a probability sampling process and do not cover entire territory (Figure 1). The stocks were computed according to Eq. 1 but since no RM data were available in BDSOL2009-2013, we used the predicted values from the RM map. The predicted OC_s values at the location of the profiles were extracted and compared to observed values (Figure 10). We found a relatively good aggreement for croplands. In grasslands and vineyards, the prediction accuracy is difficult to assess because of the lack of observations. In forests, four observations were markedly under-predicted. The main source of error for these profiles was due to an under-estimation of their OC content (predicted OC was ca. 20 g C kg^{-1} while observed OC were $>$ 35 g C kg^{-1}), which propagated in BD predictions through the use of a PTF. We have shown that OC content is difficult to predict in forest soils due its large small-scale spatial variability and the possible influence of human factors (e.g. land use history) that the models did not take into account [1] which resulted in a model able to predict only the large-scale, climate-induced variations in OC content in GDL (Table 7).

6 Conclusion

We have produced a map of OC stocks in the 0-30 cm layer which can be used to assess the amount of carbon stored in the soils of different ecosystems in GDL. Due to lack of data with OC stocks, it was not possible to develop a spatial model OC stocks directly. Instead, we combined spatial layers of OC content, bulk density (predicted through a PTF with OC as independent variable) and rock mass. The resulting map of OC stocks reflects therefore mainly variations related to the surface OC content and OC stocks prediction errors are highly related to OC content prediction errors. We found relatively large prediction errors in forests, pointing out the difficulty of mapping OC stocks due to their large spatial variability (requiring a lot of observations) and the relatively complex interplay of human and natural variables controlling the balance of OC in soils. We should note however that the predicted pixel values represent the average OC stocks under given environmental conditions. While these predictions can not always match the actual observed values at the center of the pixels, they are probably more valid when aggregated over larger areas.

References

[1] Antoine Stevens, Bas van Wesemael, Simone Marx, and Lionel Leydet. Mapping topsoil organic carbon content in grand-duchy of luxembourg. Technical report, Ministère de l'Agriculture, de la Viticulture et de la Protection des consommateurs, Ettelbruck, Luxembourg, 2014.

[1] This excludes areas that were not mapped, e.g. urban areas. The mapped area is 87% of the GDL territory, see [1].

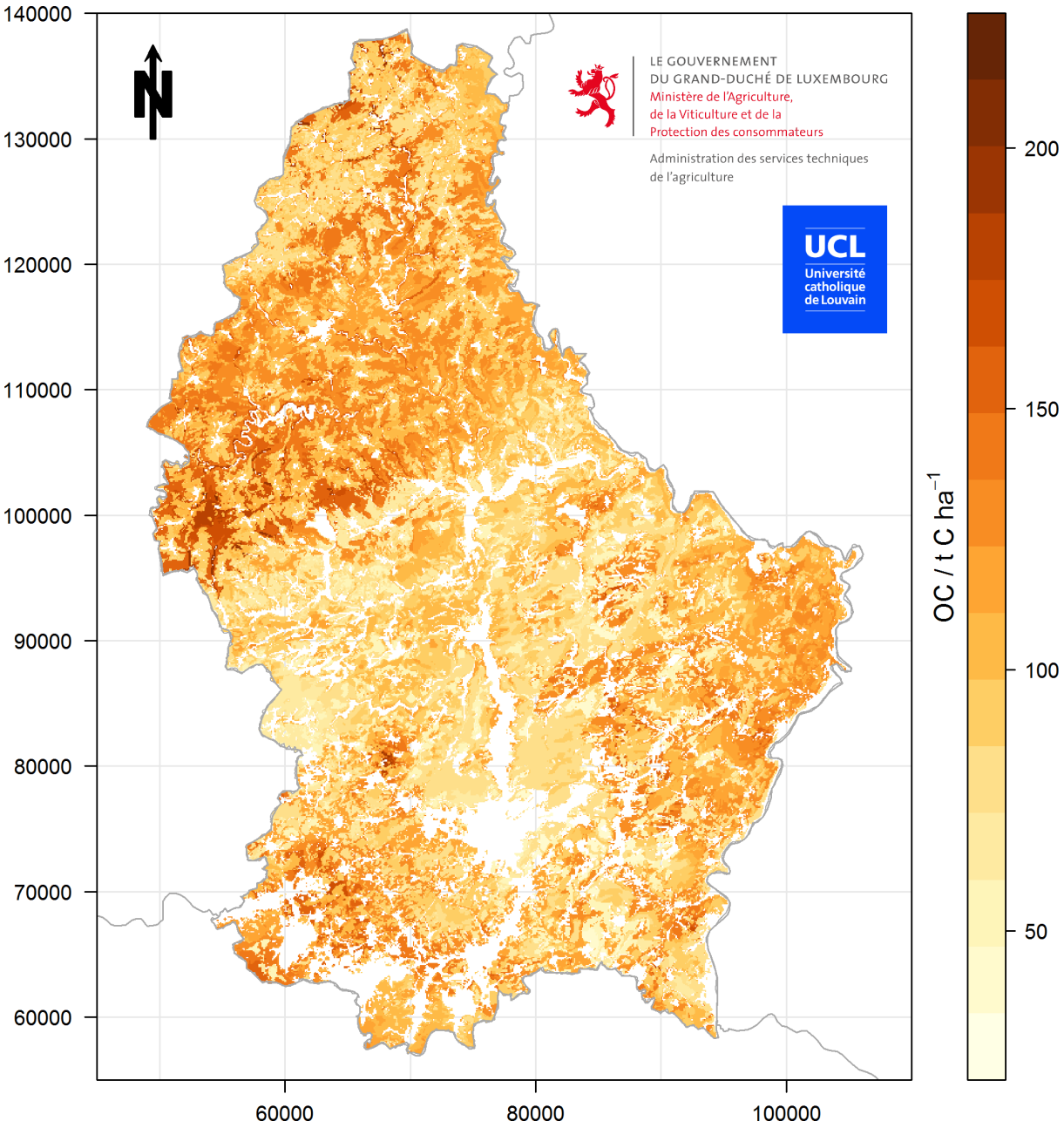

Figure 7: Map of predicted OC stocks in the 0-30 cm layer (/ t C ha^{-1}) in GDL. Areas in white corresponds to environments where no predictions could be made.

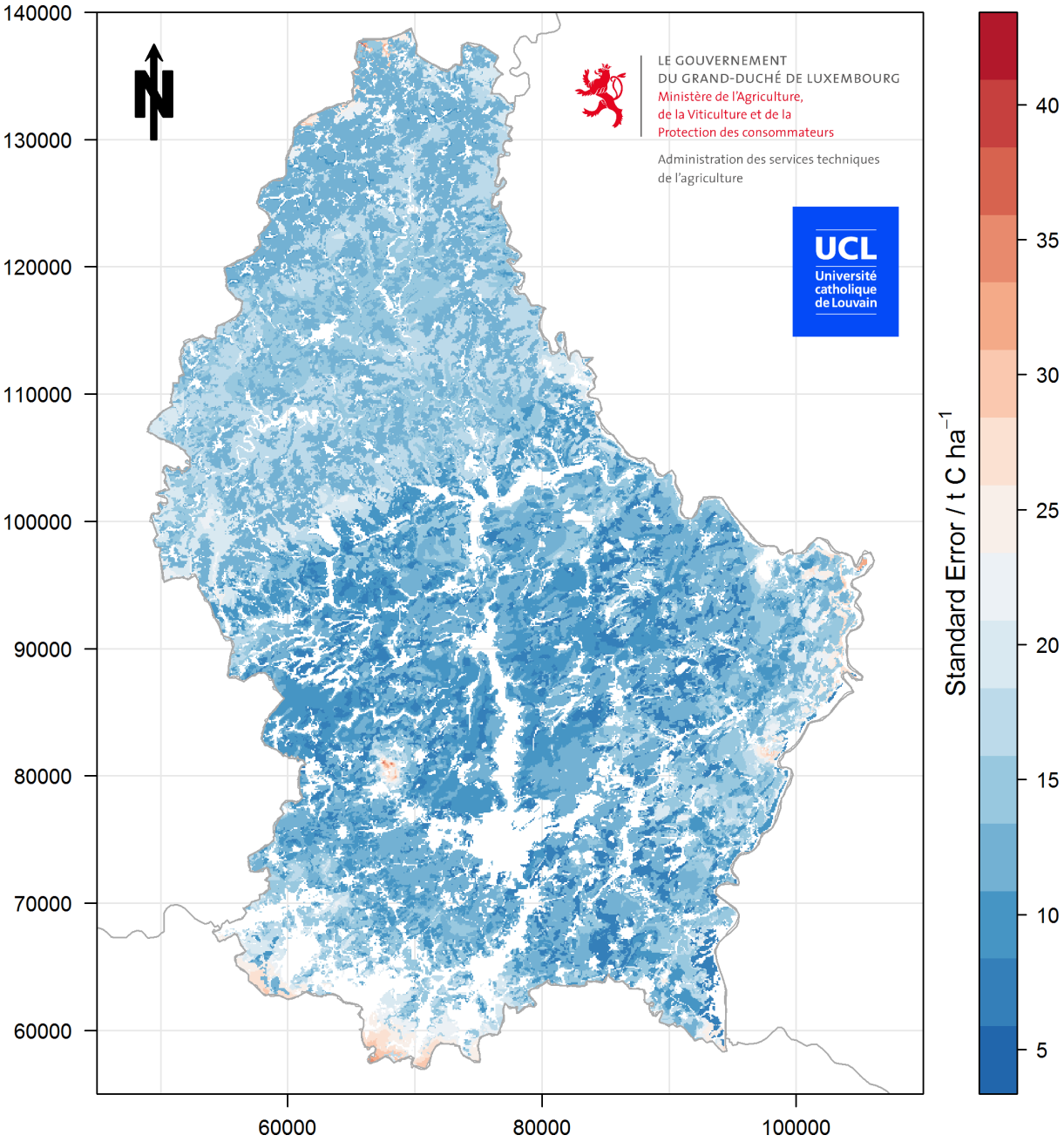

Figure 8: Map of the standard error of predicted OC stocks in the 0-30 cm layer (/ t C ha^{-1}) in cropland soils.

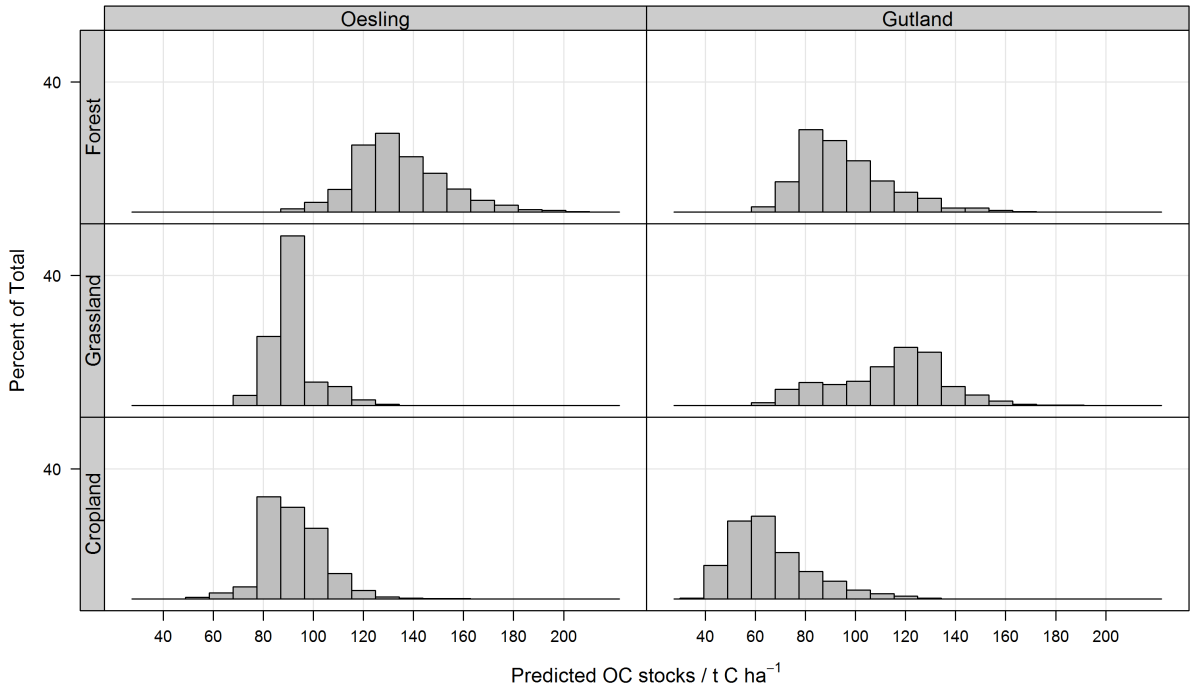

Figure 9: Histogram of values shown in the map of OC stocks in the 0-30 cm layer (/ t C ha^{-1}) in GDL soils.

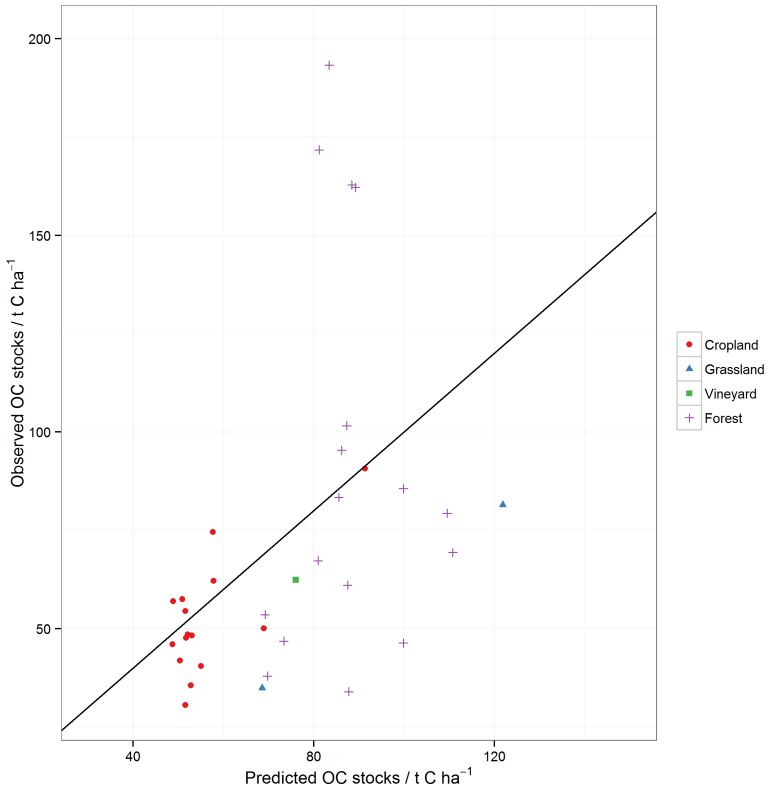

Figure 10: Predicted OC stocks (/ t C ha^{-1}) *vs* observed OC stocks in the 0-30 cm layer for the 4 land cover classes. The black line is the 1:1 line.

[2] R. Hiederer. Distribution of organic carbon in soil profile data. *Luxembourg: Office for Official Publications of the European Communities, EUR*, 23980, 2009.

[3] J. Meersmans, B. van Wesemael, F. De Ridder, and M. Van Molle. Modelling the three-dimensional spatial distribution of soil organic carbon (SOC) at the regional scale (flanders, belgium). *Geoderma*, 152(1–2):43–52, August 2009.

[4] B. Kempen, D. J. Brus, and J. J. Stoorvogel. Three-dimensional mapping of soil organic matter content using soil type–specific depth functions. *Geoderma*, 162(1–2):107–123, April 2011.

[5] B. P. Malone, A. B. McBratney, B. Minasny, and G. M. Laslett. Mapping continuous depth functions of soil carbon storage and available water capacity. *Geoderma*, 154(1–2):138–152, December 2009.

[6] T. F. A. Bishop, A. B. McBratney, and G. M. Laslett. Modelling soil attribute depth functions with equal-area quadratic smoothing splines. *Geoderma*, 91(1–2):27–45, August 1999.

[7] Tomislav Hengl, Bas Kempen, Gerard Heuvelink, Brendan Malone, and Hannes Reuter. GSIF: Global soil information facilities, 2014.

[8] Bruno De Vos, Marc Van Meirvenne, Paul Quataert, Jozef Deckers, and Bart Muys. Predictive quality of pedotransfer functions for estimating bulk density of forest soils. *Soil Science Society of America Journal*, 69(2):500–510, 2005.

[9] W. A. Adams. The effect of organic matter on the bulk and true densities of some uncultivated podzolic soils. *Journal of Soil Science*, 24(1):10–17, March 1973.

[10] Walter Rawls, J. Estimating soil bulk density from particle size analysis and organic matter content. *Soil Science*, 135(2):123–125, 1983.

[11] S. Lettens, J. Van Orshoven, B. van Wesemael, and B. Muys. Soil organic and inorganic carbon contents of landscape units in belgium derived using data from 1950 to 1970. *Soil Use and Management*, 20(1):40–47, 2004.

[12] M. Schrumpf, E. D. Schulze, K. Kaiser, and J. Schumacher. How accurately can soil organic carbon stocks and stock changes be quantified by soil inventories? *Biogeosciences*, 8(5):1193–1212, May 2011.

[13] E. Goidts, B. Van Wesemael, and M. Crucifix. Magnitude and sources of uncertainties in soil organic carbon (SOC) stock assessments at various scales. *European Journal of Soil Science*, 60(5):723–739, 2009.

A Summary of the GAM models

Table 2: Summary of the GAM models for croplands

	Full model	Reduced model
(Intercept)	2.79***	2.79***
elevation	6.03***	5.91***
eastness	1.63**	
northness	0.00	
slope	0.00	
precipitation	2.45***	3.21***
temperature	7.03***	6.25***
C factor	3.13***	3.06***
clay	2.94***	2.95***
Livestock intensity	1.83*	
LS factor	1.83*	
path length	3.42**	
x,y	12.59***	12.25***
AIC	3921.83	3951.92
BIC	4123.03	4111.63
Log Likelihood	-1916.02	-1940.32
Deviance	13521.76	14566.66
Deviance explained	0.74	0.72
Dispersion	22.20	23.56
R^2	0.72	0.71
GCV score	2007.57	2015.08
Num. obs.	653	653
Num. smooth terms	12	6

$^{***}p < 0.001$, $^{**}p < 0.01$, $^{*}p < 0.05$

Table 3: Summary of the GAM models for grasslands

	Full model	Reduced model
(Intercept)	3.25***	3.24***
elevation	0.81**	
eastness	0.77*	
northness	0.77	
slope	0.00	
precipitation	0.00	
temperature	0.21	
C factor	0.89**	
clay	0.95***	0.94***
Livestock intensity	0.00	
x,y:Oesling	0.00	1.38
x,y:Gutland	4.63**	5.08**
hydrological class†:Oesling	0.55	0.78*
hydrological class†:Gutland	0.92***	0.90**
AIC	1243.39	1256.07
BIC	1283.21	1291.29
Log Likelihood	-609.18	-616.97
Deviance	9785.53	10680.15
Deviance explained	0.42	0.37
Dispersion	58.78	63.60
R^2	0.39	0.34
GCV score	626.68	631.77
Num. obs.	178	178
Num. smooth terms	13	5

$^{***}p < 0.001$, $^{**}p < 0.01$, $^{*}p < 0.05$

Table 4: Summary of the GAM models for forests

	Full model	Reduced model
(Intercept)	3.51***	3.47***
elevation	1.37*	
eastness	0.00	
northness	0.35	
slope	1.40*	
precipitation	3.90***	4.29***
temperature	0.00	
clay	0.94***	0.95***
LS factor	0.01	
path length	2.92***	
x,y:Oesling	5.13***	5.32***
x,y:Gutland	6.84***	8.76***
AIC	4494.13	4504.65
BIC	4601.77	4596.90
Log Likelihood	-2222.19	-2231.01
Deviance	91717.34	94649.61
Deviance explained	0.53	0.51
Dispersion	171.07	175.38
R^2	0.51	0.50
GCV score	2268.14	2271.16
Num. obs.	560	560
Num. smooth terms	11	4

$^{***}p < 0.001$, $^{**}p < 0.01$, $^{*}p < 0.05$

B Summary of predicted OC stock values

Soil associations	n	Min	q_1	$\bar{x}$	$\tilde{x}$	q_3	Max	IQR
Oesling	26753	48.5	83.3	91.5	90.6	98.8	159.0	15.6
Buntsandstein	4373	43.2	59.3	66.7	63.8	69.4	136.4	10.2
Dolomies du Muschelkalk	3746	49.3	72.0	85.5	84.0	96.7	136.9	24.7
Calcaires du Bajocien	310	53.8	64.1	75.2	77.7	83.3	117.9	19.2
Grès de Luxembourg	6038	34.0	45.7	50.7	50.2	54.7	80.7	9.1
Dépôts limoneux sur Grès	7581	36.5	50.0	58.6	57.2	62.7	143.5	12.8
Argiles du Lias inf. et moyen	10333	40.6	59.5	69.8	67.7	77.9	133.8	18.5
Argiles lourdes du Keuper	4629	40.7	56.3	67.7	65.4	74.9	153.3	18.6
Argiles lourdes des schistes bitumineux	1535	52.2	67.5	88.2	89.2	107.6	126.7	40.2
Autres	2313	39.2	60.0	80.7	72.2	103.3	177.1	43.3
all	67611	34.0	60.0	76.8	78.1	91.4	177.1	31.4

Table 5: Summary statistics of OC stock predictions (t C ha-1) in Cropland

Soil associations	n	Min	q_1	$\bar{x}$	$\tilde{x}$	q_3	Max	IQR
Oesling	18775	60.7	86.2	89.2	89.8	92.1	118.5	5.9
Buntsandstein	3626	56.5	75.7	82.8	79.4	89.1	148.3	13.4
Dolomies du Muschelkalk	5299	68.3	99.1	112.1	116.0	123.9	168.5	24.9
Calcaires du Bajocien	251	91.2	115.9	122.0	119.6	128.1	149.3	12.2
Grès de Luxembourg	3574	56.6	72.7	83.3	80.0	93.3	134.7	20.5
Dépôts limoneux sur Grès	8133	65.1	85.2	99.4	96.3	111.8	191.1	26.6
Argiles du Lias inf. et moyen	14451	72.2	115.3	121.6	122.9	129.1	198.1	13.8
Argiles lourdes du Keuper	13690	68.8	110.5	121.3	124.0	130.5	175.7	20.0
Argiles lourdes des schistes bitumineux	3445	102.6	141.0	145.7	147.2	153.9	178.2	12.9
Autres	6889	60.8	102.3	110.8	113.1	121.9	191.8	19.5
all	78133	56.5	89.8	107.4	107.3	124.0	198.1	34.2

Table 6: Summary statistics of OC stock predictions (t C ha-1) in Grassland

Soil associations	n	Min	q_1	$\bar{x}$	$\tilde{x}$	q_3	Max	IQR
Oesling	42055	82.5	122.0	132.2	130.4	141.9	185.3	20.0
Buntsandstein	4901	70.3	92.1	112.1	103.0	133.4	193.5	41.3
Dolomies du Muschelkalk	4673	77.1	108.2	117.0	120.1	127.4	145.1	19.2
Calcaires du Bajocien	3030	88.5	99.5	111.5	105.2	118.0	155.3	18.5
Grès de Luxembourg	21308	57.1	75.8	80.6	80.0	84.7	165.6	8.9
Dépôts limoneux sur Grès	11903	67.3	85.2	95.7	92.6	105.4	140.4	20.2
Argiles du Lias inf. et moyen	9351	72.7	87.2	95.2	91.4	100.5	152.4	13.3
Argiles lourdes du Keuper	8160	72.3	92.8	102.6	100.0	110.8	137.6	18.1
Argiles lourdes des schistes bitumineux	3263	77.6	97.9	104.8	102.2	109.6	139.9	11.7
Autres	6296	65.2	90.0	126.6	126.2	158.9	213.2	68.9
all	114940	57.1	88.3	110.7	108.2	129.6	213.2	41.3

Table 7: Summary statistics of OC stock predictions (t C ha-1) in Forest

Soil associations	n	Min	q_1	$\bar{x}$	$\tilde{x}$	q_3	Max	IQR
Buntsandstein	57	71.0	71.0	71.0	71.0	71.0	71.0	0.0
Dolomies du Muschelkalk	556	73.5	73.5	73.5	73.5	73.5	73.5	0.0
Calcaires du Bajocien	9	77.9	77.9	77.9	77.9	77.9	77.9	0.0
Grès de Luxembourg	18	77.7	77.7	77.7	77.7	77.7	77.7	0.0
Dépôts limoneux sur Grès	15	76.2	76.2	76.2	76.2	76.2	76.2	0.0
Argiles du Lias inf. et moyen	29	75.1	75.1	75.1	75.1	75.1	75.1	0.0
Argiles lourdes du Keuper	639	75.7	75.7	75.7	75.7	75.7	75.7	0.0
Autres	334	76.0	76.0	76.0	76.0	76.0	76.0	0.0
all	1657	71.0	73.5	74.9	75.7	75.7	77.9	2.2

Table 8: Summary statistics of OC stock predictions (t C ha-1) in Vineyard

C R scripts used to generate OC stock maps

R scripts used to create a map of OC stocks in the 0-30 cm layer by combining maps of (i) OC content (g C kg^{-1}) in the 0-30 cm layer, (ii) bulk density (g cm^{-3}) as estimated by a PTF and (iii) proportion of

rock fragments in the total soil mass (g/g) can be found in the digital annex of the report. These scripts are:

1. correct_depth.r: Compute correction factor of topsoil OC content in croplands and grasslands, to represent the 0-30 cm layer, based on the BDSOL database and using mass-preserving splines to compute mean OC content over standard depths
2. gam_model_depth_corr.r: Same purpose as 'gam_model.r' but with OC corrected data
3. format_data_IFL_depth_corr.r: Same purpose as 'format_data_IFL.r' but with OC corrected data
4. attach_spatial_data_IFL_depth_corr.r: Same purpose as 'attach_spatial_data_IFL.r' but with OC corrected data
5. gam_model_depth_corr.r: Same purpose as 'gam_model.r' but with OC corrected data
6. create_OC_map_depth_corr.r: Same purpose as 'create_OC_map.r' but with OC corrected data
7. create_bd_map.r: Create a map of Bulk Density using Pedo-Transfer Rules, tested on a legacy soil profile dataset
8. create_rock_fragment_map.r: Create a map of rock fragment content in topsoils using the observed mean rock fragment content per soil association in the BDSOL database
9. create_OC_stocks_map.r: Combine maps of OC content, bulk density and proportion of rock fragment to create a OC stock map - validate the resulting map using a legacy soil profile dataset